Spectrochimica Acta Part A: Molecular and Biomolecular Spectroscopy 233 (2020) 118088

Contents lists available at ScienceDirect

Spectrochimica Acta Part A: Molecular and Biomolecular Spectroscopy

journal homepage: www.elsevier.com/locate/saa

Surface-enhanced Raman scattering as a discrimination method of *Streptococcus* spp. and alternative approach for identifying capsular types of *S. pneumoniae* isolates

S. Berus [a], E. Witkowska [a,*], K. Niciński [a], E. Sadowy [b], W. Puzia [b,c], P. Ronkiewicz [b], A. Kamińska [a,*]

[a] Institute of Physical Chemistry, Polish Academy of Sciences, Kasprzaka 44/52, 01-224 Warsaw, Poland
[b] National Medicines Institute, Chełmska 30/34, 00-725 Warsaw, Poland
[c] Institute of Biochemistry and Biophysics, Pawińskiego 5a, 02-106 Warsaw, Poland

ARTICLE INFO

Article history:
Received 13 November 2019
Received in revised form 7 January 2020
Accepted 20 January 2020
Available online 12 February 2020

Keywords:
Surface-enhanced Raman spectroscopy (SERS)
Principal component analysis (PCA)
Streptococcus spp.
Streptococcus pneumoniae
Capsular serotypes

ABSTRACT

The surface-enhanced Raman spectroscopy (SERS) is a method known for its effectiveness in detecting and identifying microorganisms, that was employed to differentiate various bacterial strains both at genus and species level. In this work, we have examined five species belonging to *Streptococcus* genus, namely *S. pneumoniae*, *S. suis*, *S. pseudopneumoniae*, *S. oralis*, and *S. mitis*. Additionally, we conducted SERS experiments on ten *S. pneumoniae* strains, representing different capsular types. In all of cases we obtained unique SERS signals being spectroscopic fingerprints of bacterial strains tested. Moreover, the principal component analysis (PCA) was performed in order to prove that the spectra of all studied strains can be well separated into five (in case of streptococcal strains) or ten (in case of pneumococcal serotypes) groups. In both investigated situations, the separation at the level of 95% was achieved, proving that SERS-PCA-based method can be used for reliable and fast identification of different strains belonging to the *Streptococcus* genus, including encapsulated pneumococcal isolates.

© 2020 Published by Elsevier B.V.

1. Introduction

Surface-Enhanced Raman Scattering (SERS) is a spectroscopic method based on the inelastic scattering of incident light by molecules absorbed on roughened metal substrate (SERS substrate) [1]. There are two main effects responsible for the enhancement of Raman signal. The first one, known as electromagnetic mechanism (EM), is related to the amplification of incident light by resonance of localized surface plasmon in the metal substrate, while the second, called chemical enhancement, relates to charge transfer (CT) excitation between the molecular orbital of the adsorbate and the Fermi level of the metal substrate. Although the enhancement factor (EF) connected with CT effect is quite low (it can reach the level up to 10^3), the EF in EM can be much stronger, with the value up to 10^{12} observed for single molecules [2,3]. In order to obtain SERS signal of measured analyte, the presence of specific metal substrate is needed. The majority of solid SERS substrates consist of Ag, Au, or Cu nanostructures [4–6], however the method applying colloids of SERS-active metals is still very popular [7–9].

Since SERS is known as noninvasive, nondestructive, reliable, ultrasensitive, and label-free method [10], it is widely used in many fields *e.g.*, catalysis [11,12], analytics [13,14], and biochemical studies [15]. A small amount of analyte required in the single experiment and no need of laborious sample preparation for measurements make SERS very promising analytical technique. Of equal importance is the fact that water, which is a main component of biological systems, is a weak Raman scattered and does not coincide with the spectrum of this kind of samples [16]. As the result, over the last decade, the interest in detection and identification of numerous proteins, cancer cells, viruses or fungi [17–23] by SERS has increased significantly. It has been also demonstrated that SERS has numerous applications in identification and detection of various bacterial species [24–29], including important pathogens causing infections in humans, *e.g. Streptococcus pneumoniae*.

S. pneumoniae is Gram-positive, alpha-hemolytic streptococcus that may be the cause of many infections such as: otitis media, pneumonia, sepsis, rhinitis, sinusitis, arthritis, conjunctivitis, and peritonitis. It is also responsible for bacterial meningitis, mostly in the elderly and children.

Meningitis, the inflammation of the protective membranes around the spinal cord and brain, may be caused by numerous types of bacteria, viruses and other microorganisms [30–32], however *Neisseria meningitidis* and *Streptococcus pneumoniae* are responsible for majority of bacterial cases in Europe [33]. Considering high fatality rates (19–35% of all cases reported only for meningitis caused by

* Corresponding authors.
E-mail addresses: ewitkowska@ichf.edu.pl (E. Witkowska), akamin@ichf.edu.pl (A. Kamińska).

https://doi.org/10.1016/j.saa.2020.118088
1386-1425/© 2020 Published by Elsevier B.V.

S. pneumoniae [34]), long-term sequela and difficulties in diagnosis, there is a continuous need for finding effective and fast detection method of bacteria in body fluids (*e.g.* cerebrospinal fluid or saliva), as well as developing identification technique at species and strain level.

Polysaccharide capsule represents a principal virulence determinant of. *S. pneumoniae* as it protects the bacteria from the immune system of the host and interferes with host opsonophagocytic clearance mechanisms [35]. For this reason non-encapsulated strains are mostly avirulent [36].

The investigation of the capsule led to identification of approximately 100 capsular serotypes of *S. pneumoniae*, however only seven of them, namely 4, 6B, 9V, 14, 18C, 19F and 23F were responsible for the vast majority of invasive pneumococcal diseases (IPD) in children in US before pneumococcal conjugate vaccine (PCV) implementation in 2000 (PCV7, Prevenar®, Pfizer) [37]. As a consequence, the incidence of IPD decreased significantly [38], nonetheless, the incidence of disease caused by non-vaccine serotypes has increased. This phenomenon is known as serotype replacement. For this reason, the PCV containing antigens present in the PCV7, as well as additional antigens characteristic for serotypes 1, 5, 7F and serotypes 1, 3, 5, 6A, 7F and 19A were licensed in 2009 as PCV10 and PCV13, respectively. This, however, does not change the fact that serotype replacement is still an ongoing process [39]. Thus, the identification of different serotypes of *S. pneumoniae* in fast and reliable manner is a topic of great importance.

The detection and identification of *S. pneumoniae* at serotype level is not the only issue appearing while examination of body fluids. Human saliva is a habitat of different harmless bacterial commensals, the large part of which is taxonomically assigned to *Streptococcus* genus [40,41]. Thus, the differentiation between *S. pneumoniae* and other closely related streptococci, such as *S. pseudopneumoniae*, *S. oralis*, and *S. mitis* is also a subject of utmost significance. Unfortunately, the standard identification procedure based on *16S rRNA* gene sequencing does not allow for identification at species level of many microorganisms, *e.g.* of some strains of salivary microbiota. Therefore, new methods enabling bacteria discrimination in precise and rapid manner is extremely needed.

In this study we present the SERS technique coupled with PCA (principal component analysis) as a method of differentiation of bacterial strains belonging to *Streptococcus* genus. Interestingly, it was also demonstrated that polysaccharide capsule can give contribution to the SERS spectrum of tested microorganism and thus enables identification of pneumococci even at serotype level.

2. Materials and methods

2.1. Bacteria species

S. mitis 3705/04, *S. oralis* 5905/12, *S. pseudopneumoniae* 6178/12, *S. suis* 2309/00, and eleven strains of *S. pneumoniae* belonging to serotypes 1 (1912/08), 3 (103/03), 4 (986/07), 5 (2706/00), 6B (9862/11), 7F (861/11), 9V (2992/05), 14 (3436/00), 19A (two strains, 5855/09 and 6394/16, of different ribosomal sequence types), and 23F (9596/11) were obtained from the National Reference Centre for Bacterial Meningitis (NRCBM) in the National Medicines Institute (NMI) in Warsaw, Poland.

2.2. Storage, culture media and conditions of bacteria cultivation

Cultures of all bacterial strains were stored at −70 °C in BBL trypticase soy broth with lysed horse blood supplemented with glycerol. In order to multiply bacterial cells, they were transferred *via* inoculation loop and incubated at 37 °C for 16 h on Columbia blood agar. All culture media were purchased from Becton Dickinson GmbH (Heidelberg, Germany).

2.3. Sample preparation for SERS measurements

Each tested bacterial colony was selected from Columbia blood agar *via* inoculation loop and placed into 100 μL of 0.9% NaCl solution (saline solution) and mixed. Next, the solution was centrifuged for 3 min at 1070 ×*g*. Subsequently, the supernatant was discarded, the new portion of saline solution was added, and the sample was mixed and centrifuged once again. This procedure was repeated three times. Finally, the purified pellet of bacterial cells was resuspended in 15 μL of 0.9% NaCl solution. About 5 μL of obtained mixture was placed over freshly prepared SERS substrate and measured after 5 min using Bruker's Bravo spectrometer.

2.4. Instrumentation

2.4.1. SERS spectroscopy

In this study the technique of dispersive Raman spectroscopy with proprietary fluorescence rejection was applied. The measurements were performed using Bruker's BRAVO spectrometer equipped with Duo LASER™ (700–1100 nm) and CCD camera. The laser power was <100 mW for both LASERs and the spectral resolution was 2–4 cm^{-1}. The SERS measurements were recorded repeatedly to obtain 25 single measurements for each investigated bacterial strain.

2.4.2. Scanning electron microscopy (SEM)

SEM measurements were performed under high vacuum using the FEI Nova NanoSEM 450. The accelerating voltage was in range from 2 kV to 10 kV.

2.5. SERS substrates preparation

In order to obtain SERS substrates, roughened silicon wafers were covered with silver. For this purpose, polished, p-doped silicon wafers of crystallographic structure (100) were etched in 30% KOH solution for 50 min at 50 °C in a specially designed reactor. Once the etching process was completed, the wafers were removed from reactor chamber and immediately placed in a baker filled with distilled water. Afterwards, they were washed under a stream of distilled water. In the next step the plates were rinsed using acetone, isopropyl alcohol, and distilled water, respectively. After all cleaning steps the platforms were dried in the flow of analyzed nitrogen and sputtered with 100 nm of silver *via* Physical Vapor Deposition (PVD) method. For this step analyzed 4 N silver target was used and the metal deposition was performed in 10^{-2} mBar vacuum using Quorum Q150T ES with 25 mA current and rotation stage.

2.6. Collection of the SERS and Raman spectra

All the spectra were processed *via* OPUS software, ver.2012 (Bruker Optic Gmbh, Germany). Spectra were smoothed using Savitsky Golay Filter (13 points) and normalized using Min-Max normalization. The background was removed using baseline correction (method: Concave rubberband correction, number of iterations: 10, number of baseline points: 64). All the spectra presented in this study were averaged from about 25 single measurements. The time required for completing a single SERS spectrum was approximately 45 s.

3. Results and discussion

The SEM imaging was used in order to study the morphology of silicon/Ag SERS substrates (see Fig. 1a–b). The silver grains with sizes ranging from 30 to 100 nm, which were covering the silicon plates, allowed to achieve the enhancement of Raman signal of all investigated bacterial strains. The repeatability of SERS measurements was depicted in Fig. 1c–d. As can be observed, all the spectra obtained for definite bacterial strain are very similar regardless of the place on the SERS platform

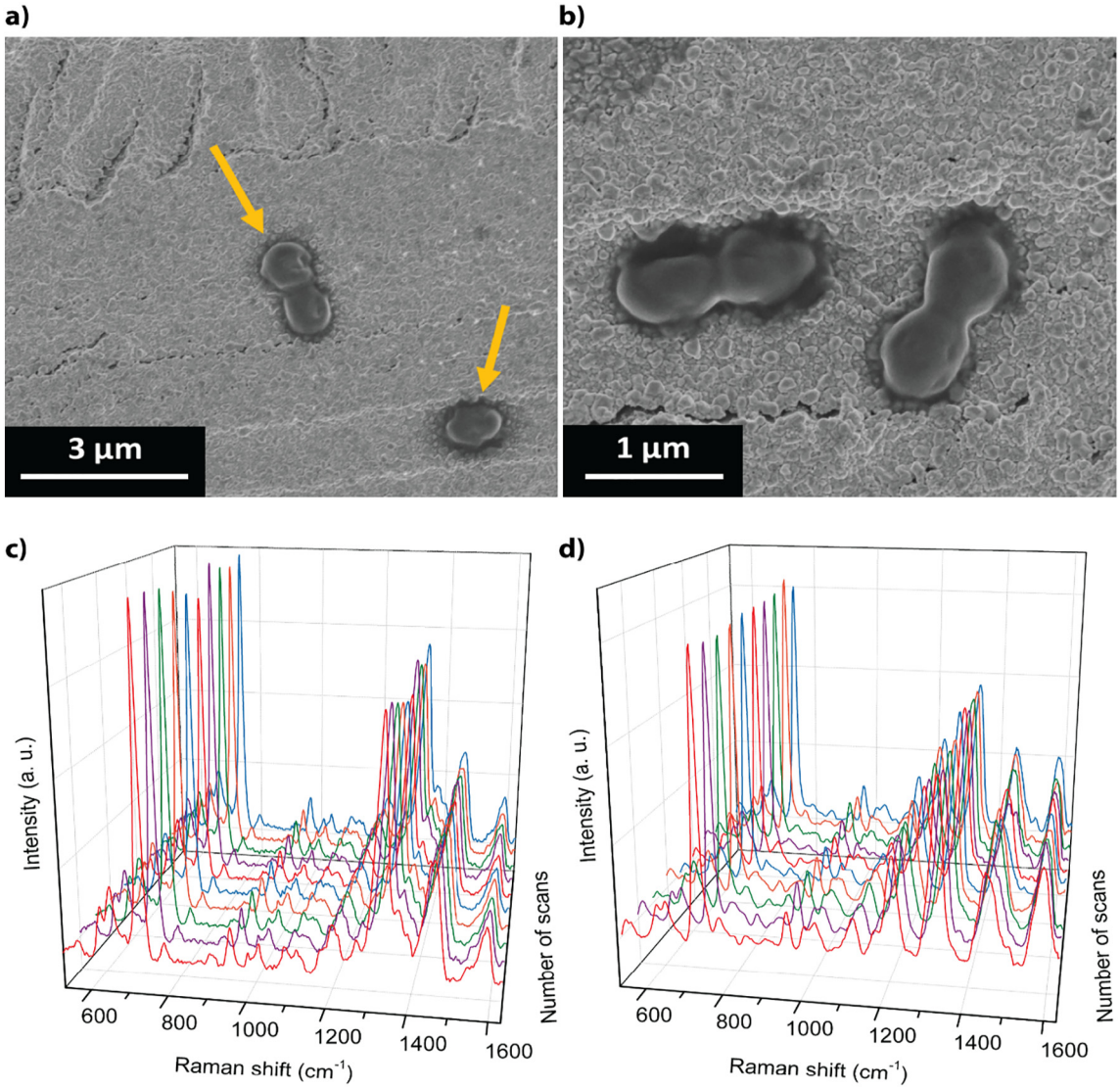

Fig. 1. SEM images of *S. pneumoniae* serotype 4 cells adsorbed to the silicon/Ag platform at different magnifications (a, b; yellow arrows in image a indicate bacterial cells) and 3D plots showing reproducibility of SERS measurements of *S. pneumoniae* serotype 4 (c) and *S. pseudopneumoniae 6178/12* (d) on silicon/Ag SERS substrates; for better visualization, only ten spectra of both strains were plotted.

in which the measurement was performed. This fact indicates that the silicon/Ag SERS substrate exhibits a high degree of homogeneity.

The colonies of five different bacterial species, all belonging to *Streptococcus* genus, were tested *via* SERS technique. Their SERS spectra in the range from 530 to 1630 cm^{-1} are shown in Fig. 2a. The spectroscopic image of all investigated streptococci is dominated mainly by the bands assigned to the oscillations in the metabolites of purine degradation, *e.g.* guanine, adenine, adenosine monophosphate (AMP), xanthine, hypoxanthine, and uric acid [42]. As a result, one can observe bands at around 730 cm^{-1} and 1330 cm^{-1} attributed to adenine/AMP and to CH_3, CH_2 wagging, respectively, as well as the band at 655 cm^{-1} which most probably comes from guanine and/or xanthine. Additionally, bacterial cell wall components, *e.g.* phospholipids and proteins, also reveal themselves in the spectrum. They appear in the form of additional bands or as changes in intensities of already existing spectroscopic features [24].

A multivariate technique called principal component analysis (PCA) was performed in order to show similarities and differences between the SERS spectra of five streptococcal species, all cultured on the same medium – Columbia blood agar. The PCA is a statistical procedure that reduces the dimensionality of complex data. In all Raman techniques, the PCA is associated with a linear transformation of spectra into a new coordinate system. Importantly, in PCA the Raman and SERS spectra are considered as N-dimensional vectors, where N is the number of data points in a single spectrum. As the result of transformation, from many wavenumber assignments one can obtain only few principal components (PCs) - the linear combinations of the original variables showing the directions along which the variations in the data are maximal. The PCs are ordered according to how much of the variations present in the data they contain. Consequently, the first principal component has the largest possible variance and each succeeding component has the highest variance possible under the restriction that it is orthogonal to the previous component(-s). In the present study, the chemometric analysis was done for the fingerprint region: 600–1600 cm^{-1}. In Fig. 2b it was demonstrated that the first principal component (PC-1) is responsible for 80% of group separation, while the first three principal components (PC-1, PC-2, and PC-3) explain together 95% of the variance in the data. These results show the possibility of differentiation of strains belonging to the same genus with a very high accuracy. Additionally, the loadings of PC-1 were plotted in the function of wavenumber (Fig. 2c). The analysis of received plot leads to the information about the most significant diagnostic variables responsible for group separation. Such

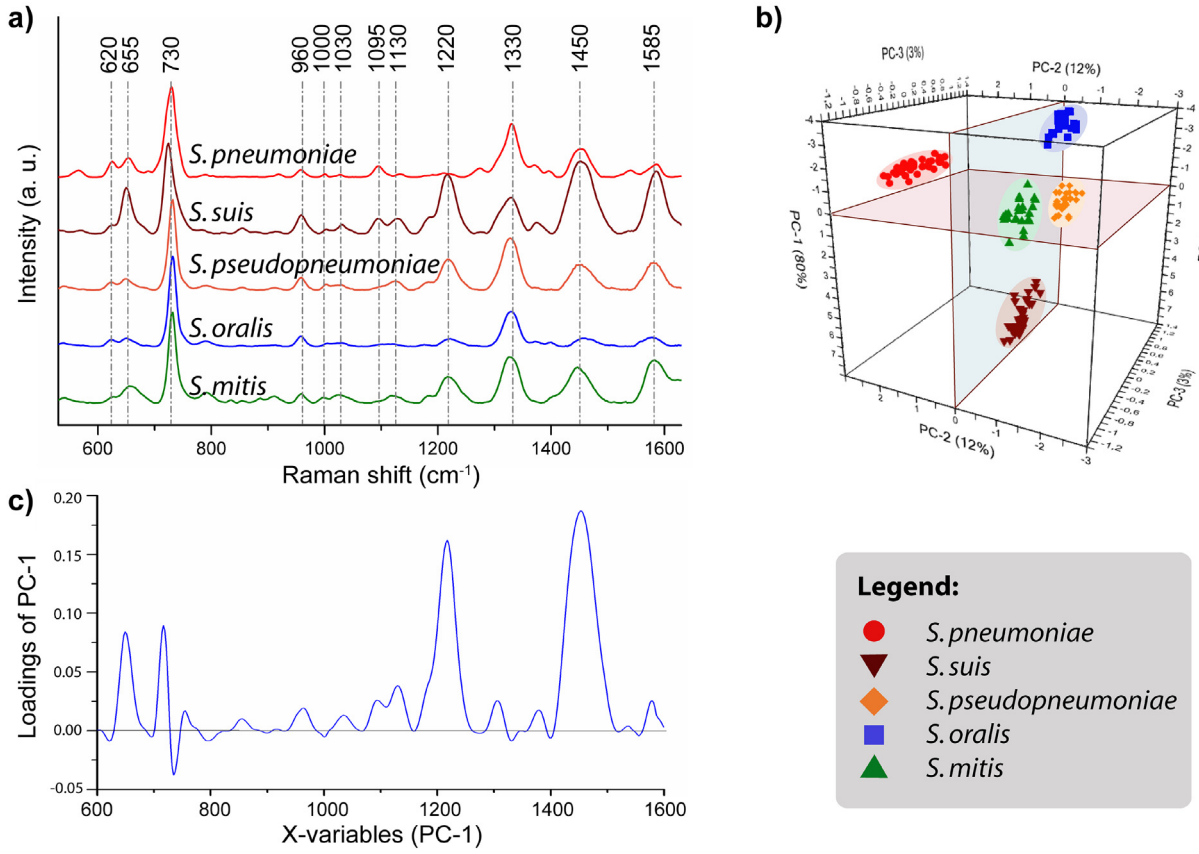

Fig. 2. The SERS spectra (a), PCA (b), and loadings plot (c) obtained for spectroscopic data of five streptococci species: *S. pneumoniae*, *S. suis*, *S. pseudopneumoniae*, *S. oralis*, and *S. mitis*. The presented spectra were measured on silicon/Ag SERS platform and averaged from at least 25 SERS measurements. Before measurements, all bacteria strains were cultured on Columbia blood agar medium for 16 h at 37 °C.

variables, indicated by the highest loadings values, were attributed to the bands at *ca.* 1220 and 1450 cm^{-1} which are assigned to amide III (random)/thymine vibrations and to CH_2 deformations, respectively.

The loading 1220 is strictly related to the wavelength and has one of the highest weight in differentiation for *S. pneumoniae* (lack of this band in the SERS spectrum). Therefore, the scores cluster corresponding to *S. pneumoniae* is separated from the others. The loading 1450 highly influences the *S. oralis* calculated scores (the lowest intensity in the SERS signature). Additionally, the SERS bands of 1450 cm^{-1} is observed in all analyzed bacterial spaces. Therefore, *S. oralis*, *S. pseudopneumoniae*, *and S. mitis* scores are positioned in the same region. It should be highlighted that the bands at 1220 and 1450 cm^{-1} for *S. suis* revealed the highest intensities and corresponding scores are separated from the others group of scores.

Additionally, the SERS measurements were performed for ten different serotypes of *S. pneumoniae*: 1, 3, 4, 5, 6B, 7F, 9V, 14, 19A, and 23F. The results are presented in Fig. 3. For each investigated *S. pneumoniae* serotype, two spectra were depicted: one averaged from at last 25 SERS measurements done in different spots of SERS substrate (spectra in Fig. 3 marked with one star), and the second obtained from single SERS measurement (spectra in Fig. 3 marked with two stars). As can be observed, these two types of spectra are very similar to each other in every case. The reason of juxtaposing these spectra was to show the reproducibility of obtained SERS results. It is also worth noting that each *S. pneumoniae* serotype exhibits its own, characteristic SERS profile (see Fig. S1, Supplementary data). For instance, the band at *ca.* 730 cm^{-1} in the case of serotype 3 has the lowest intensity compared to the same band in the spectra of other investigated serotypes, while the serotypes 7F and 23F are characterized by strong band at around 660 cm^{-1}. Other features which make each of presented spectroscopic images unique are associated with changes in intensities of the bands at 620, 1220, 1330, 1450, and 1580 cm^{-1}. The first band is assigned to C—C twisting in proteins, while the last one – to C═C bending mode in phenylalanine. For more details and precise band assignment, please see Table S1, Supplementary data.

The extensive studies of *S. pneumoniae* have revealed that there are numerous virulence factors present in pneumococcal cell surface, among which different proteins can be found. Some of these surface antigens can potentially be used as vaccine antigens as due to them the production of opsonic antibodies can be stimulated.

There are a lot of pneumococcal cell-surface proteins responsible for their virulence. Additionally, practically all pneumococcal isolates produce pneumolysin, which is a member of the family of cholesterol-dependent cytolysins and is crucial virulence factor *e.g.* in pneumonia [36]. The presence of all these biomolecules can be expressed in the SERS spectra in the form of additional bands. Furthermore, the concentration of these molecules has an influence on the intensities of observed spectroscopic signatures. This in turn gives the unique SERS signal of measured strain of *S. pneumoniae*. The scheme of pneumococcal cell including pneumococcal virulence factors is depicted in Fig. 4.

Although the pneumococcal cells are rich in various protein virulence factors, the differences observed in SERS spectra of ten investigated in this work serotypes is most probably caused by the presence of the capsule, which constitutes over a half of the entire cell volume, as it can reach the thickness of 400 nm [45]. This outermost polysaccharide layer of encapsulated *S. pneumoniae* strains is usually covalently linked to the cell wall peptidoglycan [35]. The exception from this rule are serotypes 3 and 37, and hypothetically this may be one of the reasons why the SERS spectrum of pneumococcal serotype 3 is the most distinct in comparison to other *S. pneumoniae* types.

Capsular types of *S. pneumoniae* differ in their biochemical structure – they may consist of various compounds, including saccharides,

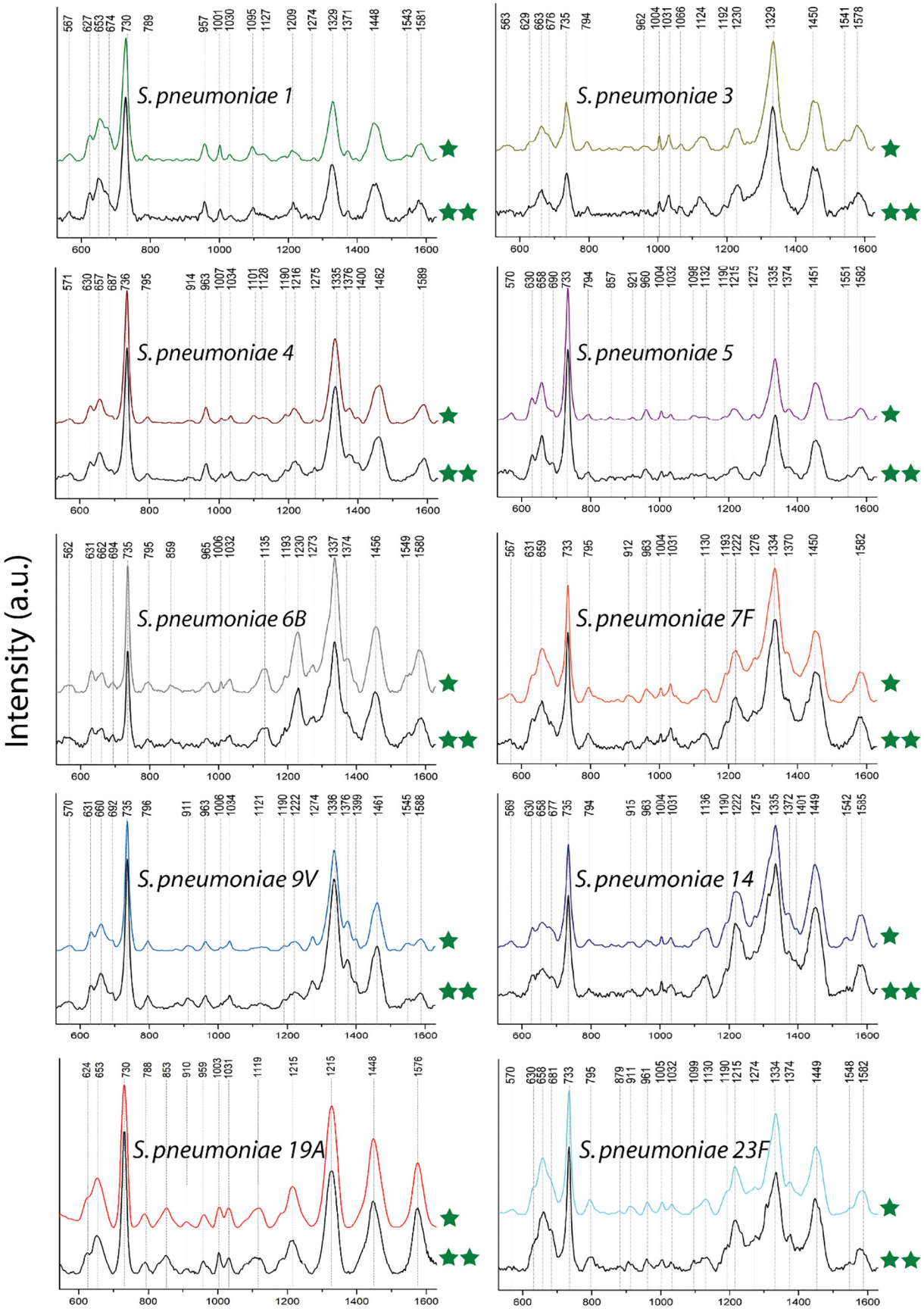
S. pneumoniae 1
S. pneumoniae 3
S. pneumoniae 4
S. pneumoniae 5
S. pneumoniae 6B
S. pneumoniae 7F
S. pneumoniae 9V
S. pneumoniae 14
S. pneumoniae 19A
S. pneumoniae 23F
Intensity (a.u.)
Raman shift (cm-1)

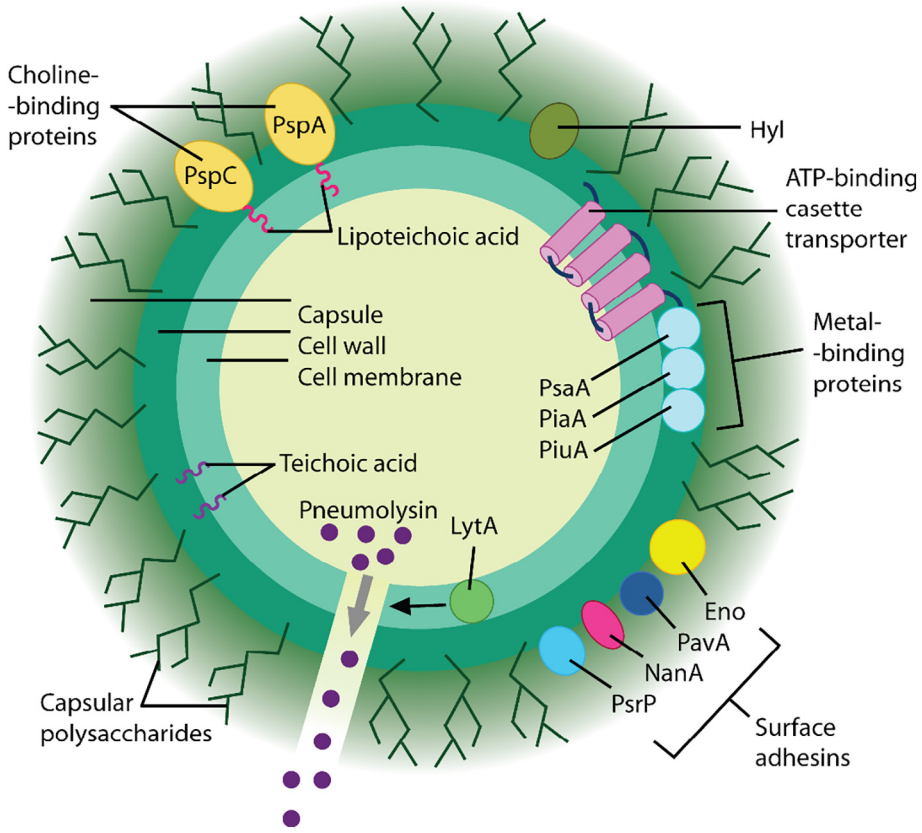

Fig. 4. The scheme representing pneumococcal cell and important pneumococcal virulence factors which include: the capsule; the cell wall; choline-binding proteins; pneumococcal surface proteins A and C (PspA and PspC); hyaluronate lyase (Hyl); pneumococcal adhesion and virulence factor A (PavA); enolase (Eno); neuraminidase A (NanA); pneumococcal serine-rich repeat protein (PsrP); pneumolysin; autolysin A (LytA); and the metal-binding proteins: pneumococcal surface antigen A (PsaA), pneumococcal iron acquisition lipoprotein A (PiaA), and pneumococcal iron uptake lipoprotein A (PiuA). The cell wall components such as lipoteichoic acid and teichoic acid are also shown.
Based on Kadioglu et al. [36], van der Poll and Opal [43], Nieto et al. [44].

alcohols, amides, *etc*. Thus, the dissimilarities between pneumococcal serotypes, which can be observed both in their SERS spectra and in PCA, are most possibly caused by the differences in the chemical composition of streptococcal capsule. In order to determine this composition, it is necessary to define the numerous structural aspects of the repeating units. This, in turn, is connected with the identification of saccharide residues, their order and linkages [46].

The repeating units of the capsule, which can be linked together in different manners, commonly consist of 2–8 saccharide residues. Additionally, the presence of phosphoglycerol, *O*-acetyl, and pyruvyl acetal substitutions was also confirmed [47]. All these features give a unique biochemical fingerprint of specific pneumococcal serotype. The fact that each capsular type has a unique structure translates into unique SERS spectrum. The structures of the capsules of ten *S. pneumoniae* serotypes investigated in this work are presented in Table 1.

There are many methods allowing to determine the serotype of encapsulated strains of *S. pneumoniae*. In order to type pneumococcal isolates, the Quellung reaction (also known as Neufeld Test) is routinely used [48]. This method is based on the reaction between antibodies and streptococcal capsule and allows visualizing positive reaction under a microscope - the capsule seems to enlarge and becomes opaque. Unfortunately, to perform this reaction, costly antisera are needed. Moreover, the method is very laborious and need experienced personnel [46]. Thus, scientists started to investigate new approaches which will allow to study the capsular types of *S. pneumoniae*, including enzyme-linked immunosorbent assay [49,50], dot blot [51], latex agglutination test [52], matrix-assisted laser desorption ionization–time of flight mass spectrometry [53], Fourier transform infrared spectroscopy [54], as well as nuclear magnetic resonance (NMR) [55]. Unfortunately, almost all of mentioned techniques are time-consuming, need very expensive equipment, or, in some cases, are insufficient to affiliate the streptococcal serotype in correct manner.

Due to biochemical differences between capsular types of pneumococci, the SERS-based approach, which is known as very sensitive spectroscopic technique, seemed to be the appropriate method allowing for differentiation of ten serotypes of *S. pneumoniae*. The obtained SERS results were used to perform PCA. The 2D and 3D PCA results, presented in Fig. 5(a–b), enabled to divide the investigated strains into ten separate groups. The PC-1 together with PC-2 explained 91% of variability, and together with PC-3 reached the value of 95%. The loadings plot of PC-1 for the whole fingerprint region is shown in Fig. 5c. As one can see, the most important diagnostic variables in the analyzed data set are located at 1220, 1330 and 1450 cm^{-1}. Moreover, we performed PCA including SERS results obtained for additional pneumococcal strain belonging to 19A serotype (5855/09) in order to demonstrate its resemblance to the strain of the same serotype (6394/16). Although the mentioned strains are attributed to the same serotype, they belong to different ribosomal sequence types, rST589 and rST11365, respectively. As one can observe in the Fig. S2 (Supplementary data), these two strains are in the close proximity to each other in PCA plots, which is due to the fact that their SERS spectra are very similar (Fig. S3a, Supplementary data). Despite this, they still can be

Fig. 3. The SERS spectra of investigated *S. pneumoniae* serotypes measured on silicon/Ag SERS platform. Each plot presents SERS spectrum averaged from at least 25 single measurements (marked with one star) and spectrum from single measurement for comparison (marked with two stars). Before measurements, all bacteria strains were cultured on Columbia blood agar medium for 16 h at 37 °C.

Table 1
The biochemical structures of ten investigated *S. pneumoniae* serotypes.

Serotype[a]	Structure[b]
1	→3)-α-AATGal*p*-(1 → 4)-α-D-Gal*p*A$2_{0.3}$,3$_{0.3}$Ac$_2$-(1 → 3)-α-D-Gal*p*A-(1→
3	→3)-β-D-Glc*p*A-(1 → 4)-β-D-Glc*p*-(1→
4	→3)-β-D-Man*p*NAc-(1 → 3)-α-L-Fuc*p*NAc-(1 → 3)-α-D-Gal*p*NAc-(1 → 4)-α-D-Gal*p*2,3(S)Pyr-(1→
5	→4)-β-D-Glc*p*A-(1→4)-α-L-Fuc*p*NAc-(1→3)-β-D-Sug*p*-(1→ 3 ↑ 1 α-L-Pne*p*NAc-(1→2)-β-D-Glc*p*A
6B	→2)-α-D-Gal*p*-(1 → 3)-α-D-Glc*p*-(1 → 3)-α-L-Rha*p*-(1 → 4)-D-Rib-ol-(5 → P→
7F	→6)-α-D-Gal*p*-(1→3)-β-L-Rha*p*2Ac-(1→4)-β-D-Glc*p*-(1→3)-β-D-Gal*p*NAc-(1→ 2 4 ↑ ↑ 1 1 β-D-Gal*p* α-D-Glc*p*NAc-(1→2)-α-L-Rha*p*
9V	→4)-α-D-Glc*p*A$2_{0.25}$,3$_{0.55}$Ac$_2$-(1 → 3)-α-D-Gal*p*-(1 → 3)-β-D-Man*p*NAc4$_{0.09}$,6$_{1.04}$Ac$_2$-(1 → 4)-β-D-Glc*p*-(1 → 4)-α-D-Glc*p*-(1→
14	→6)-β-D-Glc*p*NAc-(1→3)-β-D-Gal*p*-(1→4)-β-D-Glc*p*-(1→ 4 ↑ 1 β-D-Gal*p*
19A	→4)-β-D-Man*p*NAc-(1 → 4)-α-D-Glc*p*-(1 → 3)-α-L-Rha*p*-(1 → P→
23F	Gro-(2→P ↓ 3 →4)-β-D-Glc*p*-(1→4)- β-D-Gal*p*-(1→4)-β-L-Rha*p*-(1→ 2 ↑ 1 α-L-Rha*p*

[a] Danish type.
[b] AATGal, 2-acetamido-4-amino-2,4,6-trideoxy-D-galactose; Ac, acetate; FucNAc, *N*-acetylfucosamine; Gal, galactose; GalA, galacturonic acid; GalNAc, *N*-acetylgalactosamine; Glc, glucose; GlcA, glucuronic acid; GlcNAc, *N*-acetylglucosamine; Gro, glycerol; ManNAc, *N*-acetylmannosamine; P, phosphate; PneNAc, *N*-acetylpneumosamine (2-acetamido-2,6-dideoxytalose); Pyr, pyruvate; Rha, rhamnose; Rib-ol, ribitol; Sug, 2-acetamido-2,6-dideoxy-xylo-hexos-4-ulose; *p*, pyranose.

separated in two different groups in PCA (Fig. S3b–c, Supplementary data).

These results prove that differences between streptococcal serotypes, connected with the biochemical structure of the capsule, are visible in the SERS spectra. This, in turn, can serve in the future as a new and fast method of serotyping *S. pneumoniae* strains.

4. Conclusions

The present work describes the SERS-PCA-based method enabling rapid identification of *Streptococcus* spp. at species level. It was shown that the differentiation of five strains belonging to five diverse streptococcal species, namely *S. pneumoniae*, *S. suis*, *S. pseudopneumoniae*, *S. oralis*, and *S. mitis*, can be achieved with very high accuracy (80% only for PC-1 and 95% for PC-1 together with PC-2 and PC-3). Additionally, SERS technique coupled with PCA allowed distinguishing bacterial cells belonging to one species (*S. pneumoniae*) but to different capsular types. The separation at the level of 95% was obtained, giving high certainty of the result.

There are few reasons of serotyping pneumococcal strains. First of all, the information about capsular type is needed to develop antipneumococcal vaccines. Additionally, the studies of the capsule of *S. pneumoniae* isolates may lead to further improvement of a method for treating patients suffering from pneumococcal diseases. Finally, the serotyping procedure serve for basic epidemiological surveillance. For abovementioned reasons, the new methods enabling the determination of the serotype of pneumococcal isolates are extremely desired.

The advantages of SERS technique such as fast and label free sample preparation, or obtaining the result within few seconds perhaps will contribute to the development of the SERS-based classification of the capsular types of pneumococcal isolates and the use of this method in microbiological laboratories. In the future, we plan to continue the measurements on clinical samples, namely saliva, sputum, pharyngeal swab, nasopharyngeal swab, and tonsil swab to transfer the developed approach in the clinic diagnosis. When analyzing clinical/environmental samples in which we do not expect bacteria in normal conditions (*e.g.* urine, blood plasma, cerebrospinal fluid) the detection can be done directly from the investigated fluid [29,56]. However, in more complex samples, such as saliva, first we have to multiply bacteria on agar plates and then we select bacteria of morphology characteristic for the species we are interested in. The detection is easier in the situations when there are many colony forming units (cfu) per 1 mL (~10^2–10^3 cfu/mL). This happens when we deal with the clinical samples from ill patients. In such situation a bacterial colony can be transferred almost directly from agar plate to SERS substrate and measured within seconds.

CRediT authorship contribution statement

S. Berus: Data curation, Investigation. **E. Witkowska:** Writing - original draft. **K. Niciński:** Conceptualization. **E. Sadowy:** Resources. **W. Puzia:** Resources. **P. Ronkiewicz:** Validation. **A. Kamińska:** Writing - review & editing, Supervision.

Declaration of competing interest

The authors declare that they have no known competing financial interests or personal relationships that could have appeared to influence the work reported in this paper.

Acknowledgments

Authors thank for the financial support from Foundation for Polish Science under grant Team-Tech/2017-4/23 (POIR.04.04.00-00-4210/17-00). The study was partially financed by the grant UMO-2016/21/B/NZ7/01076 from the National Science Centre, Poland and Specjalne Urządzenie Badawcze (SPUB) MIKROBANK 2 from the Polish Ministry of Science and Higher Education.

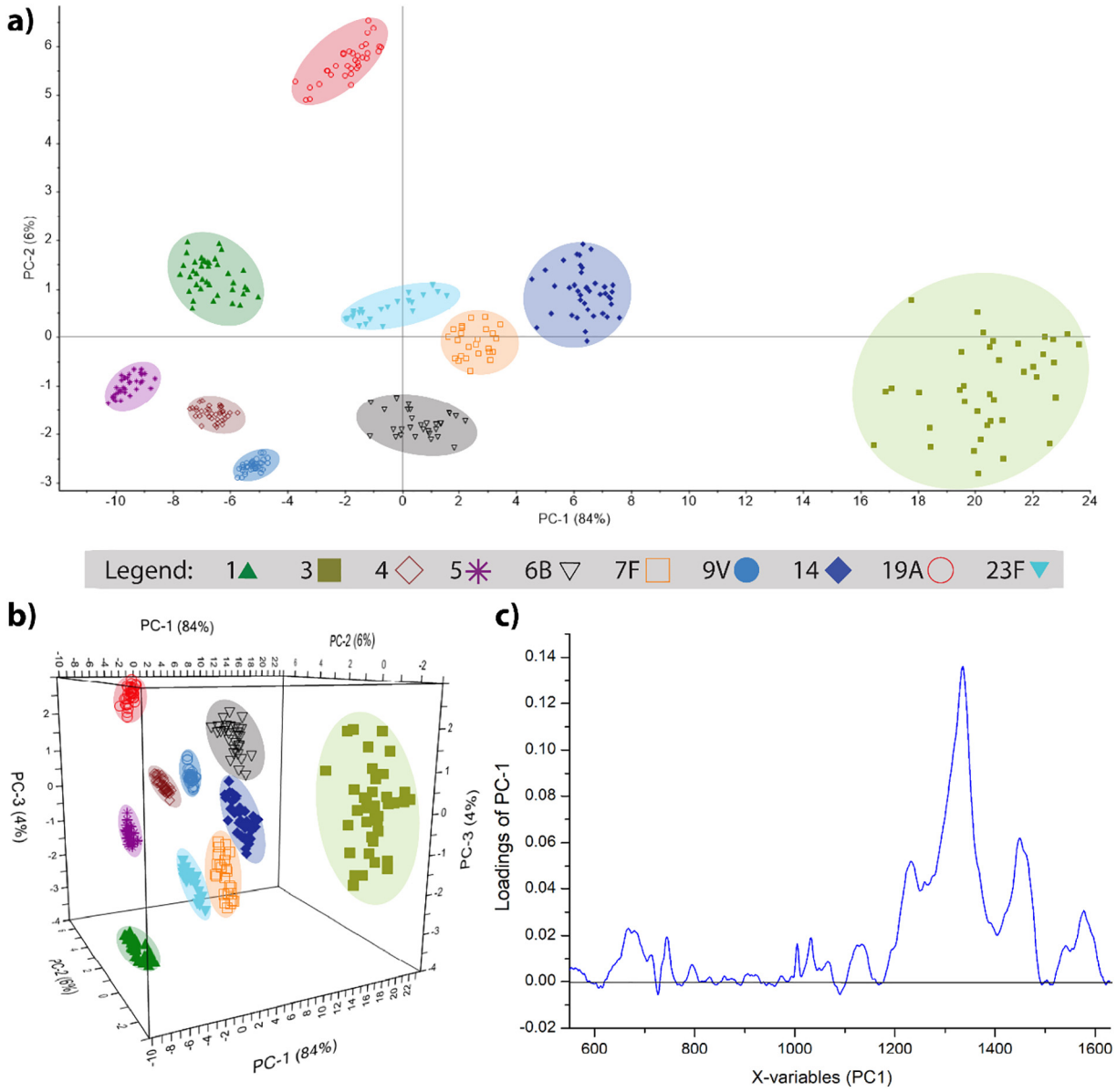

Fig. 5. The PCA results obtained for ten *S. pneumoniae* serotypes: 1, 3, 4, 5, 6B, 7F, 9V, 14, 19A, and 23F; PCA 2D (a), PCA 3D (b), and loadings plot of PC-1 (c). In order to perform PCA, at least 25 single measurements of one type of sample were done. Before measurements, all bacteria strains were cultured on Columbia blood agar medium for 16 h at 37 °C.

Appendix A. Supplementary data

Supplementary data to this article can be found online at https://doi.org/10.1016/j.saa.2020.118088.

References

[1] S. Nie, S.R. Emory, Probing single molecules and single nanoparticles by surface-enhanced Raman scattering, Science (New York, N.Y.) 275 (1997) 1102–1106.
[2] J.P. Camden, J.A. Dieringer, Y. Wang, D.J. Masiello, L.D. Marks, G.C. Schatz, R.P. Van Duyne, Probing the structure of single-molecule surface-enhanced Raman scattering hot spots, J. Am. Chem. Soc. 130 (2008) 12616–12617.
[3] E.C. Le Ru, E. Blackie, M. Meyer, P.G. Etchegoin, Surface enhanced Raman scattering enhancement factors: a comprehensive Study, J. Phys. Chem. C 111 (2007) 13794–13803.
[4] A.A. Kowalska, A. Kaminska, W. Adamkiewicz, E. Witkowska, M. Tkacz, Novel highly sensitive Cu-based SERS platforms for biosensing applications, J. Raman Spectrosc. 46 (2015) 428–433.
[5] K. Niciński, E. Witkowska, D. Korsak, K. Noworyta, J. Trzcińska-Danielewicz, A. Girstun, A. Kamińska, Photovoltaic cells as a highly efficient system for biomedical and electrochemical surface-enhanced Raman spectroscopy analysis, RSC Adv. 9 (2019) 576–591.
[6] R. Bardhan, N.K. Grady, J.R. Cole, A. Joshi, N.J. Halas, Fluorescence enhancement by au nanostructures: nanoshells and nanorods, ACS Nano 3 (2009) 744–752.
[7] R.G. Freeman, K.C. Grabar, K.J. Allison, R.M. Bright, J.A. Davis, A.P. Guthrie, M.B. Hommer, M.A. Jackson, P.C. Smith, D.G. Walter, M.J. Natan, Self-assembled metal colloid monolayers: an approach to SERS substrates, Science (New York, N.Y.) 267 (1995) 1629–1632.
[8] K.C. Grabar, R.G. Freeman, M.B. Hommer, M.J. Natan, Preparation and characterization of au colloid monolayers, Anal. Chem. 67 (1995) 735–743.
[9] J. Neddersen, G. Chumanov, T.M. Cotton, Laser ablation of metals: a new method for preparing SERS active colloids, Appl. Spectrosc. 47 (1993) 1959–1964.
[10] S. Cui, S. Zhang, S. Yue, Raman spectroscopy and imaging for cancer diagnosis, J. Healthc. Eng. 2018 (2018) 11.
[11] R. Liu, J.-F. Liu, Z.-M. Zhang, L.-Q. Zhang, J.-F. Sun, M.-T. Sun, G.-B. Jiang, Submonolayer-Pt-coated ultrathin Au nanowires and their self-organized nanoporous film: SERS and catalysis active substrates for operando SERS monitoring of catalytic reactions, J. Phys. Chem. Lett. 5 (2014) 969–975.
[12] L. Cui, X. Ren, X. Yang, P. Wang, Y. Qu, W. Liang, M. Sun, Plasmon-driven catalysis in aqueous solutions probed by SERS spectroscopy, J. Raman Spectrosc. 47 (2016) 877–883.
[13] S.M. Restaino, I.M. White, A critical review of flexible and porous SERS sensors for analytical chemistry at the point-of-sample, Anal. Chim. Acta 1060 (2019) 17–29.

[14] A.I. Radu, O. Ryabchykov, T.W. Bocklitz, U. Huebner, K. Weber, D. Cialla-May, J. Popp, Toward food analytics: fast estimation of lycopene and beta-carotene content in tomatoes based on surface enhanced Raman spectroscopy (SERS), Analyst 141 (2016) 4447–4455.
[15] E. Garcia-Rico, R.A. Alvarez-Puebla, L. Guerrini, Direct surface-enhanced Raman scattering (SERS) spectroscopy of nucleic acids: from fundamental studies to real-life applications, Chem. Soc. Rev. 47 (2018) 4909–4923.
[16] J. De Gelder, K. De Gussem, P. Vandenabeele, L. Moens, Reference database of Raman spectra of biological molecules, J. Raman Spectrosc. 38 (2007) 1133–1147.
[17] A.F. Chrimes, K. Khoshmanesh, S.Y. Tang, B.R. Wood, P.R. Stoddart, S.S. Collins, A. Mitchell, K. Kalantar-zadeh, In situ SERS probing of nano-silver coated individual yeast cells, Biosens. Bioelectron. 49 (2013) 536–541.
[18] A. Kamińska, E. Witkowska, K. Winkler, I. Dzięcielewski, J.L. Weyher, J. Waluk, Detection of hepatitis B virus antigen from human blood: SERS immunoassay in a microfluidic system, Biosens. Bioelectron. 66 (2015) 461–467.
[19] A. Szeghalmi, S. Kaminskyj, P. Rösch, J. Popp, K.M. Gough, Time fluctuations and imaging in the SERS spectra of fungal hypha grown on nanostructured substrates, J. Phys. Chem. B 111 (2007) 12916–12924.
[20] E. Witkowska, T. Jagielski, A. Kaminska, A. Kowalska, A. Hryncewicz-Gwozdz, J. Waluk, Detection and identification of human fungal pathogens using surface-enhanced Raman spectroscopy and principal component analysis, Anal. Methods 8 (2016) 8427–8434.
[21] S. Feng, S. Huang, D. Lin, G. Chen, Y. Xu, Y. Li, Z. Huang, J. Pan, R. Chen, H. Zeng, Surface-enhanced Raman spectroscopy of saliva proteins for the noninvasive differentiation of benign and malignant breast tumors, Int. J. Nanomedicine 10 (2015) 537–547.
[22] S. Feng, R. Chen, J. Lin, J. Pan, G. Chen, Y. Li, M. Cheng, Z. Huang, J. Chen, H. Zeng, Nasopharyngeal cancer detection based on blood plasma surface-enhanced Raman spectroscopy and multivariate analysis, Biosens. Bioelectron. 25 (2010) 2414–2419.
[23] K. Zhang, C. Hao, B. Man, C. Zhang, C. Yang, M. Liu, Q. Peng, C. Chen, Diagnosis of liver cancer based on tissue slice surface enhanced Raman spectroscopy and multivariate analysis, Vib. Spectrosc. 98 (2018) 82–87.
[24] E. Witkowska, D. Korsak, A. Kowalska, A. Janeczek, A. Kamińska, Strain-level typing and identification of bacteria – a novel approach for SERS active plasmonic nanostructures, Anal. Bioanal. Chem. 410 (2018) 5019–5031.
[25] S. Efrima, L. Zeiri, Understanding SERS of bacteria, J. Raman Spectrosc. 40 (2009) 277–288.
[26] C. Fan, Z. Hu, A. Mustapha, M. Lin, Rapid detection of food- and waterborne bacteria using surface-enhanced Raman spectroscopy coupled with silver nanosubstrates, Appl. Microbiol. Biotechnol. 92 (2011) 1053–1061.
[27] R.M. Jarvis, A. Brooker, R. Goodacre, Surface-enhanced Raman scattering for the rapid discrimination of bacteria, Faraday Discuss. 132 (2006) 281–292(discussion 309-219).
[28] A. Kaminska, E. Witkowska, A. Kowalska, A. Skoczynska, P. Ronkiewicz, T. Szymborski, J. Waluk, Rapid detection and identification of bacterial meningitis pathogens in ex vivo clinical samples by SERS method and principal component analysis, Anal. Methods 8 (2016) 4521–4529.
[29] E. Witkowska, T. Szymborski, A. Kamińska, J. Waluk, Polymer mat prepared via Forcespinning™ as a SERS platform for immobilization and detection of bacteria from blood plasma, Mater. Sci. Eng. C 71 (2017) 345–350.
[30] S.A.E. Logan, E. MacMahon, Viral meningitis, BMJ 336 (2008) 36–40.
[31] O. Hoffman, R.J. Weber, Pathophysiology and treatment of bacterial meningitis, Ther. Adv. Neurol. Disord. 2 (2009) 1–7.
[32] C.B. Treseler, A.M. Sugar, Fungal meningitis, Infect. Dis. Clin. N. Am. 4 (1990) 789–808.
[33] A.M. Oordt-Speets, R. Bolijn, R.C. van Hoorn, A. Bhavsar, M.H. Kyaw, Global etiology of bacterial meningitis: a systematic review and meta-analysis, PLoS One 13 (2018) e0198772.
[34] D. van de Beek, J. de Gans, A.R. Tunkel, E.F. Wijdicks, Community-acquired bacterial meningitis in adults, N. Engl. J. Med. 354 (2006) 44–53.
[35] J.C. Paton, C. Trappetti, Streptococcus pneumoniae capsular polysaccharide, Microbiology Spectrum 7 (2019).
[36] A. Kadioglu, J.N. Weiser, J.C. Paton, P.W. Andrew, The role of Streptococcus pneumoniae virulence factors in host respiratory colonization and disease, Nat. Rev. Microbiol. 6 (2008) 288–301.
[37] D.R. Feikin, K.P. Klugman, Historical changes in pneumococcal serogroup distribution: implications for the era of pneumococcal conjugate vaccines, Clin. Infect. Dis. 35 (2002) 547–555.
[38] M.H. Kyaw, R. Lynfield, W. Schaffner, A.S. Craig, J. Hadler, A. Reingold, A.R. Thomas, L.H. Harrison, N.M. Bennett, M.M. Farley, R.R. Facklam, J.H. Jorgensen, J. Besser, E.R. Zell, A. Schuchat, C.G. Whitney, Effect of introduction of the pneumococcal conjugate vaccine on drug-resistant Streptococcus pneumoniae, N. Engl. J. Med. 354 (2006) 1455–1463.
[39] F. Raymond, N. Boucher, R. Allary, L. Robitaille, B. Lefebvre, C. Tremblay, J. Corbeil, A. Gervaix, Serotyping of Streptococcus pneumoniae based on capsular genes polymorphisms, PLoS One 8 (2013) e76197.
[40] I. Nasidze, J. Li, D. Quinque, K. Tang, M. Stoneking, Global diversity in the human salivary microbiome, Genome Res. 19 (2009) 636–643.
[41] T. Ogawa, Y. Hirose, M. Honda-Ogawa, M. Sugimoto, S. Sasaki, M. Kibi, S. Kawabata, K. Ikebe, Y. Maeda, Composition of salivary microbiota in elderly subjects, Sci. Rep. 8 (2018) 414.
[42] W.R. Premasiri, J.C. Lee, A. Sauer-Budge, R. Theberge, C.E. Costello, L.D. Ziegler, The biochemical origins of the surface-enhanced Raman spectra of bacteria: a metabolomics profiling by SERS, Anal. Bioanal. Chem. 408 (2016) 4631–4647.
[43] T. van der Poll, S.M. Opal, Pathogenesis, treatment, and prevention of pneumococcal pneumonia, Lancet 374 (2009) 1543–1556.
[44] P.A. Nieto, S.A. Riquelme, C.A. Riedel, A.M. Kalergis, S.M. Bueno, Gene elements that regulate Streptococcus pneumoniae virulence and immunity evasion, Curr. Gene Ther. 13 (2013) 51–64.
[45] U.B. Skov Sorensen, J. Blom, A. Birch-Andersen, J. Henrichsen, Ultrastructural localization of capsules, cell wall polysaccharide, cell wall proteins, and F antigen in pneumococci, Infect. Immun. 56 (1988) 1890–1896.
[46] K.A. Geno, G.L. Gilbert, J.Y. Song, I.C. Skovsted, K.P. Klugman, C. Jones, H.B. Konradsen, M.H. Nahm, Pneumococcal capsules and their types: past, present, and future, Clin. Microbiol. Rev. 28 (2015) 871–899.
[47] J.J. Calix, R.J. Porambo, A.M. Brady, T.R. Larson, J. Yother, C. Abeygunwardana, M.H. Nahm, Biochemical, genetic, and serological characterization of two capsule subtypes among Streptococcus pneumoniae serotype 20 strains: discovery of a new pneumococcal serotype, J. Biol. Chem. 287 (2012) 27885–27894.
[48] M. Habib, B.D. Porter, C. Satzke, Capsular serotyping of Streptococcus pneumoniae using the Quellung reaction, J. Vis. Exp. (2014) e51208.
[49] J.P. Leeming, K. Cartwright, R. Morris, S.A. Martin, M.D. Smith, G. South-West Pneumococcus Study, Diagnosis of invasive pneumococcal infection by serotype-specific urinary antigen detection, J. Clin. Microbiol. 43 (2005) 4972–4976.
[50] K.S. Lankinen, S. Rintamäki, R. Syrjänen, T. Kilpi, P. Ruutu, M. Leinonen, Type-specific enzyme immunoassay for detection of pneumococcal capsular polysaccharide antigens in nasopharyngeal specimens, J. Microbiol. Methods 56 (2004) 193–199.
[51] A. Fenoll, I. Jado, D. Vicioso, J. Casal, Dot blot assay for the serotyping of pneumococci, J. Clin. Microbiol. 35 (1997) 764–766.
[52] H.C. Slotved, M. Kaltoft, I.C. Skovsted, M.B. Kerrn, F. Espersen, Simple, rapid latex agglutination test for serotyping of pneumococci (Pneumotest-Latex), J. Clin. Microbiol. 42 (2004) 2518–2522.
[53] T.C.A. Pinto, N.S. Costa, L.F.S. Castro, R.L. Ribeiro, A.C.N. Botelho, F.P.G. Neves, J.M. Peralta, L.M. Teixeira, Potential of MALDI-TOF MS as an alternative approach for capsular typing Streptococcus pneumoniae isolates, Sci. Rep. 7 (2017) 45572.
[54] R.K. Sahu, S. Mordechai, S. Pesakhov, R. Dagan, N. Porat, Use of FTIR spectroscopy to distinguish between capsular types and capsular quantities in Streptococcus pneumoniae, Biopolymers 83 (2006) 434–442.
[55] C. Abeygunawardana, T.C. Williams, J.S. Sumner, J.P. Hennessey, Development and validation of an NMR-based identity assay for bacterial polysaccharides, Anal. Biochem. 279 (2000) 226–240.
[56] T. Szymborski, E. Witkowska, W. Adamkiewicz, J. Waluk, A. Kaminska, Electrospun polymer mat as a SERS platform for the immobilization and detection of bacteria from fluids, Analyst 139 (2014) 5061–5064.